

## Preparation, characterization, and flocculation performance of P(acrylamide-co-diallyldimethylammonium chloride) by UV-initiated template polymerization

Qingqing Guan,<sup>1,2</sup> Huaili Zheng,<sup>1,2</sup> Jun Zhai,<sup>1,2</sup> Bingzhi Liu,<sup>1,2</sup> Yongjun Sun,<sup>1,2</sup> Yili Wang,<sup>3</sup> Zhinan Xu,<sup>1,2</sup> Chun Zhao<sup>1,2</sup>

<sup>1</sup>Key Laboratory of the Three Gorges Reservoir Region's Eco-Environment, Ministry of Education, Chongqing University, Chongqing 400045, China

<sup>2</sup>National Centre for International Research of Low-Carbon and Green Buildings, Chongqing University, Chongqing 400045, China

<sup>3</sup>College of Environmental Science and Engineering, Research Center for Water Pollution Source Control and Eco-remediation, Beijing Forestry University, Beijing 100083, China

Correspondence to: H. Zheng (E-mail: zhl@cqu.edu.cn) and J. Zhai (E-mail: zhaijun99@126.com)

**ABSTRACT:** This study prepared TPDA, a high-intrinsic-viscosity cationic polyacrylamide, through ultraviolet (UV)-initiated template polymerization. Acrylamide (AM) and diallyldimethylammonium chloride (DMD) served as monomers, and poly sodium polyacrylate (PAAS) served as the template. The structure of TPDA was characterized by Fourier-transform infrared spectroscopy, proton nuclear magnetic resonance spectroscopy, and thermogravimetric analysis. The synthetic conditions of TPDA were studied and optimized by single-factor experiments. An optimized product was obtained at an intrinsic viscosity of  $11.3 \text{ dL g}^{-1}$  and a conversion rate of 97.2% with a total monomer concentration of 20%, DMD concentration of 30%, initiator concentration of 0.045%, pH of 8, EDTA concentration of 0.3%, and UV irradiation of 90 min. Results showed that TPDA was the copolymer of AM and DMD with a micro-block structure at the molecular chain. Given its high intrinsic viscosity and cationic block structure, TPDA performed better in kaolin flocculation than that prepared without template addition. © 2014 Wiley Periodicals, Inc. *J. Appl. Polym. Sci.* **2015**, *132*, 41747.

**KEYWORDS:** copolymers; photopolymerization; properties and characterization; separation techniques

Received 1 September 2014; accepted 12 November 2014

DOI: 10.1002/app.41747

### INTRODUCTION

Municipal and industrial wastewaters, such as effluents of paint or chemical production industries that contain large amounts of kaolin clay, possess poor quality and pose a severe threat to underground and surface water resources.<sup>1</sup> Flocculation technology is of vital importance with a wide range of applications in water and wastewater treatment plants.<sup>2,3</sup> The performance of flocculation is largely affected by flocculants that enhance the aggregation of particles to form large, rapid-setting flocs either through charge neutralization or chain-bridging mechanisms. Polyelectrolytes with cationic charges and high molecular weights have been extensively used as flocculants for colloidal suspensions to separate and dewater solid/water systems. The cationic copolymer P[acrylamide(AM)-*co*-dimethyldiallylammonium chloride (DMD)](PDA) has the advantages of high molecular weight, high charge, good water solubility, high efficiency, nontoxicity, stable cationic structure, and wide pH range.<sup>4</sup> Moreover, PDA is cheaper than other cationic polymers in the international market.<sup>5</sup> Therefore, PDA is widely used in

oil exploitation, papermaking, wastewater treatment, mining, printing and dyeing of textiles, daily chemical industry, slurry dehydration, etc.

To produce PDA, AM and DMD have been polymerized via solution polymerization,<sup>4,5</sup> disperse polymerization<sup>6–8</sup> and inverse emulsion polymerization.<sup>9</sup> However, the aforementioned polymerization methods are limited by the random distribution of cationic units in the cationic polyacrylamide (CPAM) molecular chain. The cationic units located on the loops and tails of the chain are simply wasted as shown in Figure 1(a), whereas insufficient cationic charges are available at the adsorption sites to neutralize counter ions. By contrast, blocking the cationic units as shown in Figure 1(b) strengthens the adsorption sites between copolymer and negatively charged particle segments and makes the cationic charges efficiently utilized. Hence, the flocculation performance is increased. The syntheses of DNA and RNA yield extremely low error rates with specific base sequences obtained through template and complementary base pairing. Therefore, we infer that the preparation of PDA with a

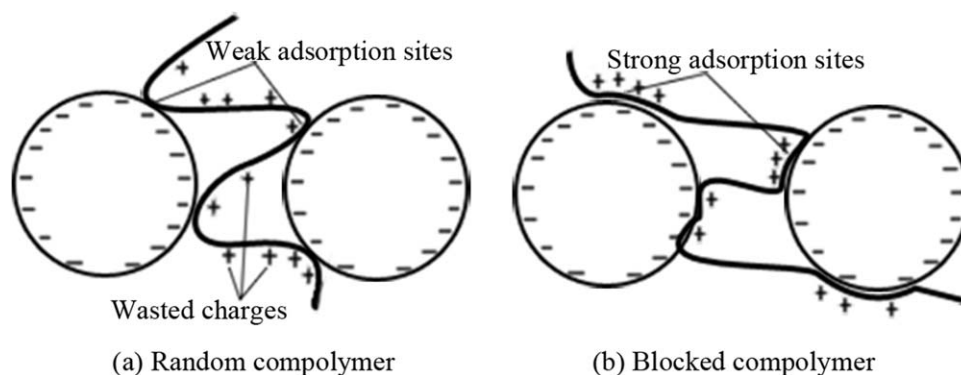


**Figure 1.** Schematic presentation of flocculation effect of a polyelectrolyte chain: (a) random copolymer and (b) cationic blocked structure copolymer.

cationic block structure can imitate the process through template or matrix polymerization, which would significantly increase flocculation efficiency.

Template copolymerization is a polymerization process in which one monomer is organized by a preformed macromolecule (template) through hydrogen or ionic bonds and another is not, and the monomers adsorbed on the template form a block structure.<sup>10</sup> Only a few studies have employed template polymerization to synthesize high-molecular-weight flocculants, most of which are ionic. A few studies have focused on the synthesis of cationic polymers, and only Charalambopoulou *et al.* synthesized cationic polymers through template polymerization when the molecular weight was only at the  $10^5$  level. To the best of our best knowledge, no previous research has used template polymerization to prepare PDA. CPAM polymerization is commonly initiated through heat, rays, microwaves, or ultraviolet (UV) waves. Our previous research indicated that UV initiation has the advantages of easy control, low reaction temperature, short polymerization time, large polymer molecular weight, and environment friendliness.<sup>11–15</sup>

The present study investigated the possibility of synthesizing TPDA flocculants through UV-initiated template polymerization. The ionic homopolymer sodium polyacrylate (PAAS) served as the template for the cationic monomer through ionic bonds. The photoinitiated copolymer TPDA was characterized through Fourier-transform infrared (FT IR) spectroscopy,  $^1\text{H}$  nuclear magnetic resonance ( $^1\text{H}$  NMR) spectroscopy, and thermogravimetric analysis (TGA). Polymer intrinsic viscosity or molecular weight was closely related to the bridging effect. An effective bridging effect often brings acceptable flocculation performance. Therefore, the effects of various preparation factors on the intrinsic viscosity and conversion of the copolymer were extensively investigated. These factors include initiator concentration (V50 and V044), monomer concentration, mass ratio between AM and DMD, pH, EDTA concentration, and irradiation time. Furthermore, the flocculation performance of TPDA was compared with that of SPDA prepared through solution polymerization in flocculating kaolin suspensions.

## EXPERIMENTAL

### Materials

The monomer AM (98.5%, w/w) was obtained from Lanjie Tap Water (Chongqing, China). The cationic monomer DMD was

supplied by Luyue Chemical (Taian, China). The template PAAS was a gift from Shandong Xintai Water Treatment (Zaozhuang, China). The photoinitiator 2,2'-azobis(2-methylpropionamide)-dihydrochloride (V50) and 2,2'-Azobis[2-(2-imidazolin-2-yl)propane] dihydrochloride (V044) were obtained from Ruihong Biological Technology (Shanghai, China). Kaolin was from Guangfu Fine Chemical Institute (Tianjin, China). The other reagents used in the experiments, including ethanol, urea [ $\text{CO}(\text{NH}_2)_2$ ], hydrochloric acid (HCl), and sodium hydroxide (NaOH), were of analytical grade. All aqueous and standard solutions were prepared with deionized water. The purity of nitrogen gas was higher than 99.99%.

### Preparation of Template Polymer

The preparation device is the same with our previous study.<sup>12</sup> The preparation of PDA was performed as follows: AM, DMD, and PAAS (mole ratio between a chain unit and DMD of 1.0) were first added to a reaction vessel made of silicate glass. Urea, which acted as the cosolvent, and EDTA, which acted as complexant and deionized water were then added to the aqueous solution. The pH value of the aqueous solution was adjusted to a specific value using sodium hydroxide and hydrochloric acid. Initiator V50 or V044 were added during the purging of nitrogen gas for 30 min prior to UV activation. Through UV-induced polymerization (main radiation wavelength between 300 and 400 nm, 365 nm; average irradiation intensity,  $2000 \mu\text{W cm}^{-2}$ ) for a specific period, the flocculant was produced, and the aqueous solution was changed into a translucent colloid. PAAS was removed after 2 h at room temperature to increase the polymerization degree. The copolymer was dissolved in water in an amount that was 10 times the weight of the copolymer. After the copolymer had been dissolved, the pH was adjusted to be  $< 2$  (30QD pH meter, HACH, Loveland, CO), and then, the dissolved copolymer was precipitated and purified with ethanol. The copolymer was then ground into powders after it had been dried for 48 h in a DZF-6021 vacuum drying oven (Shanghai, China) at  $60^\circ\text{C}$ . SPDA was prepared under similar condition with TPDA except that the template was not added. The possible reaction scheme of PDA is presented in Figure 2.

### Characterization of the Polymer

The FTIR of the copolymer and monomers were conducted using a 550 Series II infrared spectrometer (Mettler-Toledo,

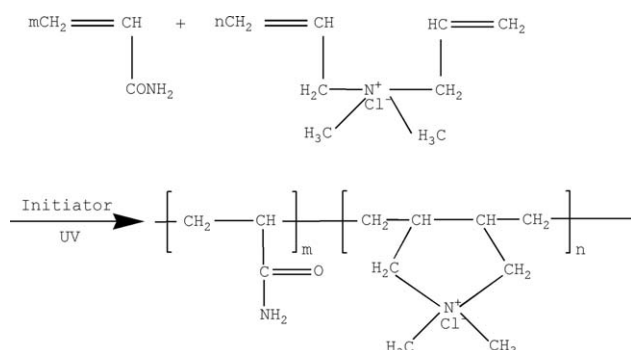


**Figure 2.** Scheme of the reaction route for the preparation of TPDA.

Greifensee, Switzerland). The interval of the measured wave numbers was from 500 to 4000  $\text{cm}^{-1}$ .

The  $^1\text{H}$  NMR spectra of the flocculant were recorded on Bruker AVANCE-500 spectrometer (Bruker Company, Karlsruhe, Germany) in  $\text{D}_2\text{O}$  solvent.

TGA was carried out at a heating rate of  $10^\circ\text{C min}^{-1}$ , a nitrogen flow rate of  $20 \text{ mL min}^{-1}$ , and a temperature range of  $20\text{--}600^\circ\text{C}$  on a DTG-60H synchronal thermal analyzer (Shimadzu, Kyoto, Japan).

The conversion and the intrinsic viscosity of PDA were determined by the gravimetric and one point method, respectively.<sup>9,11</sup> The intrinsic viscosity was expressed in deciliter per gram ( $\text{dL g}^{-1}$ ) and measured in  $1.0 \text{ mol L}^{-1}$  NaCl solution with an Ubbelohde capillary viscometer (Shanghai Shenyi Glass Instrument, China) at  $30^\circ\text{C} \pm 0.05^\circ\text{C}$ .

### Kaolin Suspension Tests

The kaolin powder was sieved through a 200-mesh sifter firstly to enable its suspension in water. The kaolin particles (0.1 wt %) in water were mostly  $<5 \mu\text{m}$ , with a mean size of about  $2.0 \mu\text{m}$ , as measured using a Winner 2000 laser particle size analyzer (Jinan Winner Particle Technology, Jinan, China). The original turbidity of the suspension was about 350 NTU. SPDA and TPDA were added to the kaolin suspension as a solution of 0.1 wt %. Flocculation experiments were conducted in a jar test using a ZR4-6 program control coagulation experiment blender (Zhongrun Water Industry Technology and Development, Shenzhen, China). The kaolin suspension was poured into beakers and was stirred at a high speed of 500 rpm for 10 min, and the flocculant solution was added immediately. The kaolin suspension was mixed at a

high speed of 500 rpm for 2 min and a low rate of 200 rpm for 2 min. After 10-min settling, the sample was located starting from 3 cm below the surface. Supernatant turbidity was measured using a 2100P turbidity meter (HACH, Loveland, USA).

## RESULTS AND DISCUSSION

### Characterization

Figure 3 shows the FTIR spectra of AM, DMD and TPDA. The adsorption peaks and corresponding structures were marked in Figure 3.<sup>16</sup> It can be seen that the adsorption peaks of  $\text{C}=\text{C}$  double bonds were disappeared in Figure 3(c). The reason is that AM and DMD reacted during UV-initiated template polymerization. However, the polymer FTIR spectrum was not the superposition of that of the monomers. Several peaks of the monomer spectra, e.g.  $1600 \text{ cm}^{-1}$  in Figure 3(a) and  $2986 \text{ cm}^{-1}$  in Figure 3(b), were disappeared in the polymer FTIR spectra. These structures transferred to infrared inactive state after polymerization because of similar vibration frequency and stringent selection law.

Figure 4 displays the  $^1\text{H}$  NMR spectra of PDA. As shown in Figure 4, the asymmetric adsorption peaks at  $\delta$  of 1.68 and 1.79 ppm can be ascribed to the protons at the backbone methylene group  $-\text{CH}_2-$  (a, c). Protons at the backbone methine group  $-\text{CH}-$  (b) of the AM unit were evidenced by the asymmetric adsorption peaks at  $\delta$  of 2.21 and 2.36 ppm. The signal at  $\delta$  of 3.82 ppm was attributed to the protons in the methine group  $-\text{CH}-$  (d) at the backbone of the DMD unit. The wide chemical shifts at  $\delta$  of 3.01–3.35 ppm were assigned to protons of  $-\text{N}^+(\text{CH}_3)_3$  (f). Protons in methylene groups  $-\text{CH}_2-$  (e) bonding with  $-\text{N}^+$  of DMD unit were exhibited at  $\delta$  of 3.79 ppm. The sharp signal at 4.78 ppm was attributed to the solvent  $\text{D}_2\text{O}$ . No obvious chemical shift was observed after 4.78 ppm indicating that almost none left monomers in the polymer.<sup>4</sup> The  $^1\text{H}$  NMR spectra further indicated that AM and DMD were polymerized.

Figure 5 shows the TGA thermograms of TPDA. Three main stages of thermal decomposition of the copolymer, corresponding to its weight reduction, can be observed. In the initial stage, the weight of PDA decreased by  $\sim 12.9\%$  (w/w) at  $30\text{--}230^\circ\text{C}$ . According to references,<sup>17,18</sup> the weight loss can be ascribed to the evaporation of intra and intermolecular moisture. These water molecules were adsorbed by the hydrophilic groups of the copolymer from the air during grinding it into powder and TGA experimental preparation process. During the second stage, the weight decreased again by  $\sim 16.0\%$  at  $230\text{--}315^\circ\text{C}$ ; this

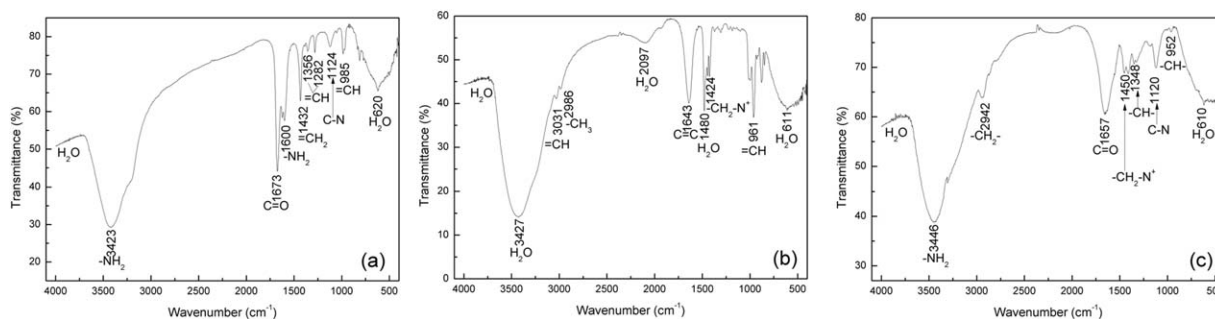


**Figure 3.** FTIR spectra of (a) AM, (b) DMD and (c) TPDA.

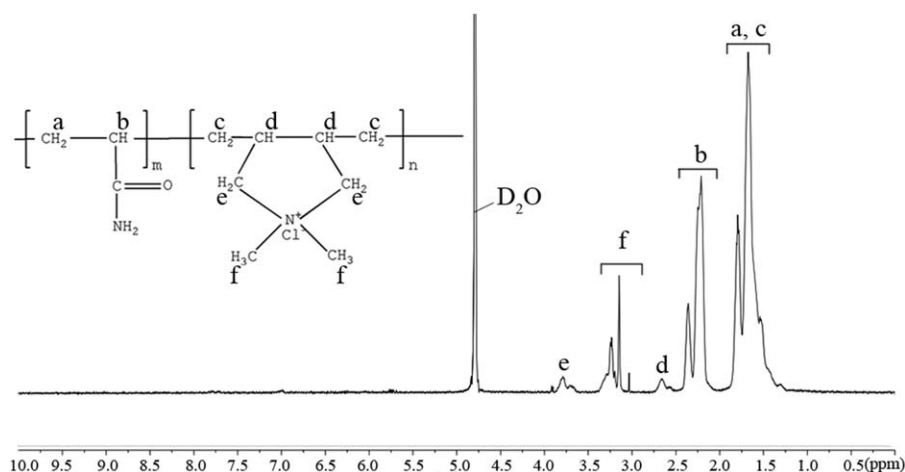


Figure 4.  $^1\text{H}$  NMR spectra of TPDA.

weight loss can be ascribed to the imidization of the amide group and the thermal decomposition of the quaternary ammonium groups. The apparent peak of heat adsorption that corresponded to the weight loss of the second stage appeared at  $284.7^\circ\text{C}$ . Meanwhile, the decomposition temperatures of TP and SP were both  $284.7^\circ\text{C}$  (Figure 5), indicating that PDA had favorable thermal stabilities. The final stage of thermal decomposition occurred above  $315^\circ\text{C}$ , with weight losses of  $\sim 50.4\%$ . These weight losses are due to the thermal decomposition of the copolymer backbone and five-membered pyrrolidinium rings. We supposed that the heat adsorption peak at  $333.4^\circ\text{C}$  can be attributed to the decomposition of the bond between the methine and methylene groups of AM units. The heat adsorptions at  $438.7$  and  $480.7^\circ\text{C}$  can be ascribed to the thermal decomposition of the backbone and five-membered pyrrolidinium rings of DMD units. The three heat adsorption peaks may provide the evidence of the cationic block structure of PDA. Only two adsorption peaks would appear if the copolymer units were randomly distributed because the heat adsorption peaks for the decomposition of the backbone methylene and methine groups would be integrated. Previous research observed similar phenomena for block structure copolymers.<sup>19</sup>

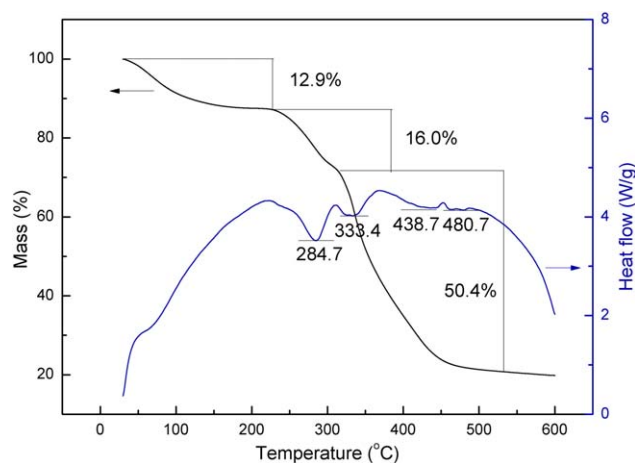


Figure 5. TGA thermograms of TPDA. [Color figure can be viewed in the online issue, which is available at [wileyonlinelibrary.com](http://wileyonlinelibrary.com).]

### Optimizing Synthesis Conditions

**Effect of Initiator V50 and V044 Concentration.** The effect of initiator V50 and V044 concentrations on polymerization was compared to select an appropriate initiator for the template polymerization system, considering the significant influence of an initiator on the chain initiation of intrinsic viscosity adjustment.<sup>11</sup> As shown in Figure 6, the intrinsic viscosity increased as the initiator concentration ranged from 0.02 to 0.04% for V044 and 0.02% to 0.06% for V50 and then decreased with excessive initiators addition, whereas the conversion constantly increased for both initiators. A potential explanation can be obtained through free radical polymerization theory because adding a template does not change the reaction mechanism.<sup>20,21</sup> At a low initiator concentration, cage effect occurred and led to a low intrinsic viscosity and conversion. This result can be attributed to the fact that a few free radicals result in the predominating termination of the growing chains inside the cage.<sup>22</sup> When the initiator concentration was increased, more and more radicals were generated, and the possibility of escaping them from their cages greatly increased. Hence, the intrinsic viscosity and conversion growth increased. During such periods, V044 showed higher intrinsic viscosity and conversion than V50

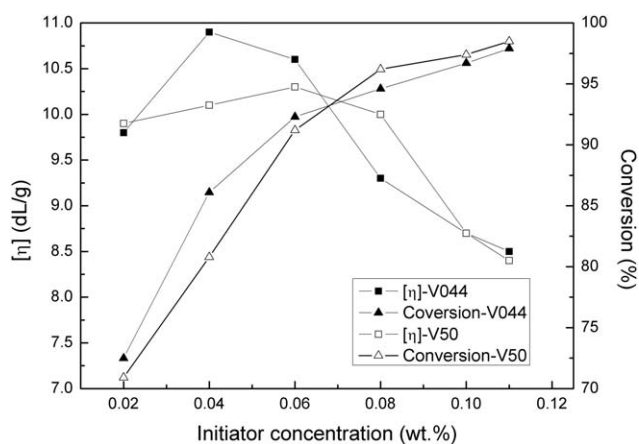
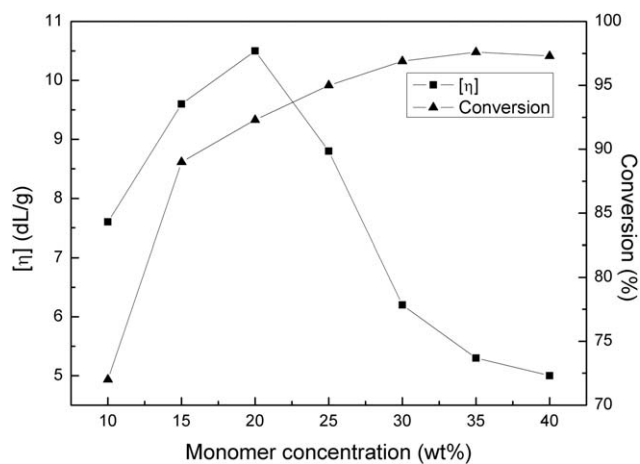


Figure 6. Effect of initiator V50 and V044 concentration on intrinsic viscosity and conversion.



**Figure 7.** Effect of monomer concentration on intrinsic viscosity and conversion.

(Figure 6). We determined that 0.06% rather than 0.04% was the appropriate concentration of the initiator V044 for TPDA polymerization reaction, considering the conversion. However, the increasing termination and chain transfer rate outweighed the increasing free radical effect, and the intrinsic viscosity decreased when the initiator concentration was above 0.04% for V044 and 0.06% for V50.

**Effect of Monomers Concentration.** Monomer concentration is a critical factor in TPDA polymerization partly because the number of free radicals is determined by monomer concentration at the start of the reaction.<sup>12</sup> As shown in Figure 7, the conversion of TPDA continuously increased in the monomer concentration range, whereas its intrinsic viscosity increased with increasing monomer concentration, peaked, and then sharply decreased. The conversion was mainly determined by the initial content of free radicals (Figure 7). However, for intrinsic viscosity, according to the free radical mechanism, less collision occurred between monomers and free radicals because the free radical production rate was slow at a low monomer concentration. The polymerization was prone to the aforementioned cage effect, which decreased polymerization and chain propagation. However, further increase enhanced heat generation and reduced thermal diffusivity, which led to the intermolecular crosslink and gel effect.<sup>23</sup>

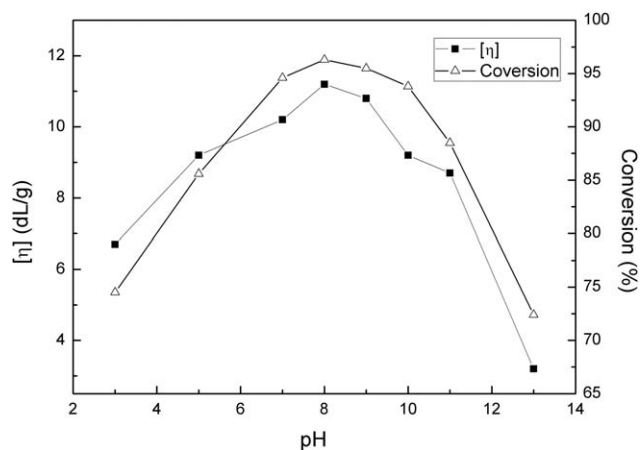


**Figure 8.** Effect of pH on intrinsic viscosity and conversion.

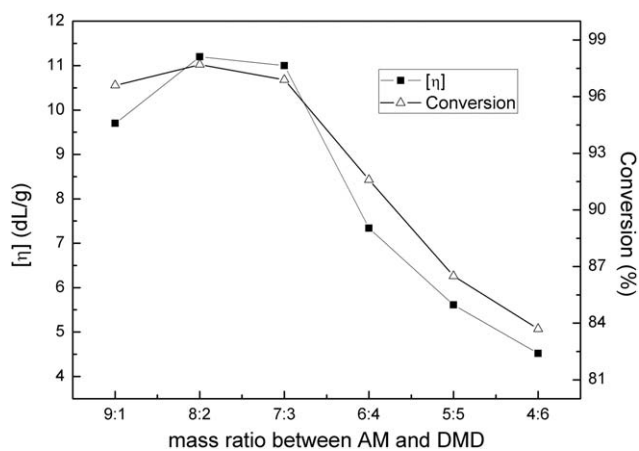


**Figure 9.** Effect of mass ratio between AM and DMD on intrinsic viscosity and conversion.

In addition, the chain transfer and chain termination accelerated and became faster than the chain propagation with decreasing intrinsic viscosity. Thus, the favorable value of monomer concentration in this study was 20.0%.

**Effect of pH.** Figure 8 illustrates the effect of pH on the intrinsic viscosity and conversion of TPDA. Results showed that both intrinsic viscosity and conversion increased with increasing pH but considerably decreased as the pH was further increased. The intermolecular and intramolecular imidization under acidic conditions led to the formation of crosslinked and branched polymers, which was the main reason for the low intrinsic viscosity. In strong alkaline conditions ( $\text{pH} > 10$ ), the amide group of AM hydrolyzed to  $\text{NH}_3$ , which further reacted with acrylamide to form nitrilotripropionamide and carbonium ion.<sup>14</sup> Nitrilotripropionamide caused polymerization termination and chain transfer, whereas the electrophile of carbonium ions inhibited polymerization, thereby forming a copolymer with low intrinsic viscosity and conversion. Accordingly, the optimum pH of 8.0 to 9.0 was adopted.

**Effect of Mass Ratio Between AM and DMD.** CPAM has wide applications because it can neutralize the surface charge of colloid particles to form large flocs. Charge density is directly related to the effectiveness of charge neutralization and the performance of flocculation. As shown in Figure 9, both the

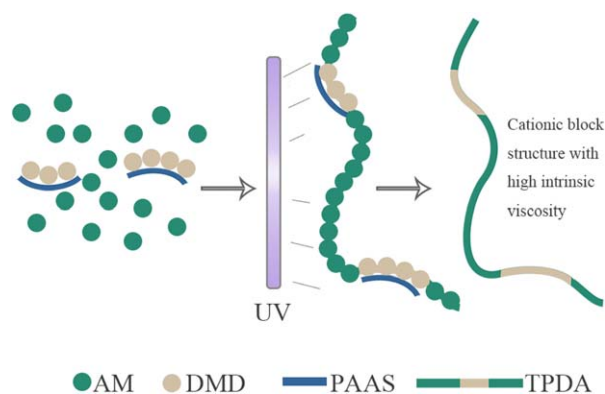


**Figure 10.** Template polymerization diagram of TPDA. [Color figure can be viewed in the online issue, which is available at [wileyonlinelibrary.com](http://wileyonlinelibrary.com).]

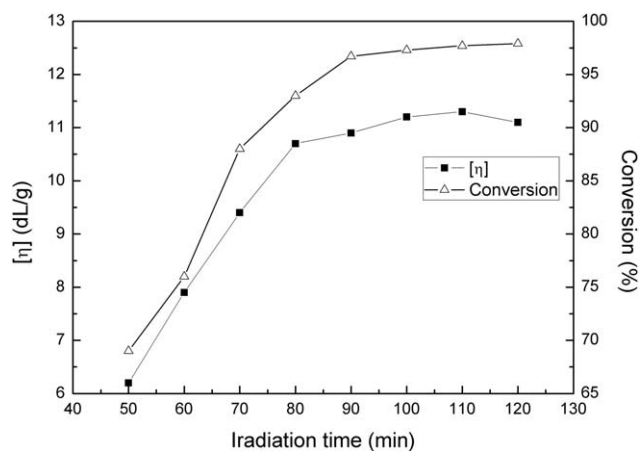


**Figure 11.** Effect of irradiation time on intrinsic viscosity and conversion.

intrinsic viscosity and polymerization conversion of TPDA marginally increased and then decreased with increasing DMD content. However, Wang *et al.* reported that intrinsic viscosity and conversion continuously decrease with increasing DMD content. At a low reactivity ratio, large steric hindrance and cationic charge repulsion of DMD decrease intrinsic viscosity.<sup>6</sup> Figure 10 shows the template polymerization diagram of TPDA. DMD was distributed along the PASS molecular chain through strong intermolecular ionic bond before polymerization, whereas AM was not. During polymerization, when a growing radical group encountered DMD adsorbed on PAAS, the DMD monomers along the template were polymerized one after another to increase its reactivity and to form cationic blocks, as indicated through TGA thermograms and as shown in Figure 10.<sup>10,24</sup> On the contrary, stochastic polymerization of DMD monomers and AM monomers were occurred for SPDA and cationic blocks cannot be formed. Consequently, the intrinsic viscosity and conversion increased or stayed stable when the mass ratio between AM and DMD ranged from 9 : 1 to 7 : 3, even though the large steric hindrance and cationic charge repulsion of DMD still functioned for TPDA. Nevertheless, the latter two effects predominated over the template effect as the DMD content was further increased. In addition, the optimum intrinsic viscosity was considerably higher in the present study than in previous studies,<sup>6,8,25</sup> which indicated the merits of adding a template. The mass ratio between AM and DMD of 7:3 was preferred, considering the charge neutralization performance of TPDA.

**Effect of Irradiation Time.** Figure 11 shows the effect of UV irradiation time on polymerization. UV irradiation can generally decompose initiator, and free radicals were generated to initiate the polymerization. In addition, Seabrook<sup>26</sup> indicated that the photo-initiated polymerization kinetics of acrylamide in water fits well with classical free-radical polymerization kinetics. Accordingly, Figure 11 shows that irradiation time significantly affected TPDA intrinsic viscosity and conversion. With prolonged illumination, intrinsic viscosity and conversion significantly improved in the first 90 min and then remained relatively stable. Thus, 90 min was selected as the optimum illumination time because this time length was enough for the polymerization to complete. Obviously, UV-initiated polymer-

ization was more favorable than thermal polymerization because the latter often takes 120 min or more to be almost completely polymerized.<sup>7</sup> Furthermore, our previous study indicated that UV-initiated polymerization can synthesize copolymers with higher intrinsic viscosity than thermal polymerization.<sup>11</sup> It might provide another explanation for the high intrinsic viscosity of  $>11.0 \text{ dL g}^{-1}$  in the present study.

**Effect of EDTA Concentration.** A small amount of metal ions such as  $\text{Fe}^{3+}$  or  $\text{Ca}^{2+}$ , which pose difficulty for preparing flocculants with high intrinsic viscosity, may exist in the polymerization system. Adding the complexant EDTA can efficiently weaken or eliminate such negative effects. As shown in Figure 12, impurities were well shielded through EDTA addition as the EDTA concentration was increased from 0.1 to 0.3%, as indicated by the uptrend of intrinsic viscosity and conversion. However, further increasing the EDTA concentration sharply decreased the intrinsic viscosity and conversion. This result can be attributed to the fact that excessive EDTA acts as a chain transfer agent in the reaction system.<sup>27</sup> Therefore, the optimal EDTA concentration was 0.3% with an intrinsic viscosity of  $11.3 \text{ dL g}^{-1}$  and a conversion of 97.2%.

#### Flocculation Performance

The effect of any flocculant on the flocculation process is influenced by the dosages, the flocculation efficiency decreasing at lower or higher dosages than the optimum dose. Turbidity, an indication of the content of suspended particle in the liquid phase, is widely used to explain the performance of a polymer sample in various flocculation fields. In this study, we determined the effect of flocculant dosage on the supernatant turbidity using TPDA and SPDA as shown in Figure 13. Both TPDA and SPDA were prepared under the aforementioned optimal conditions. The charge density of TPDA and SPDA was  $\sim 30.0 \text{ \% (wt)}$ , with intrinsic viscosities of  $11.3$  and  $9.2 \text{ dL g}^{-1}$ , respectively.

As shown in Figure 13, the residual turbidity of TPDA and SPDA sharply decreased with increasing polycation dose, reaching a minimum, and then gradually increased. This result can be ascribed to two reasons. First, the simultaneous adsorption of individual polymer chains onto several particles formed bridges between adjoining particles with floc formation when the dosage

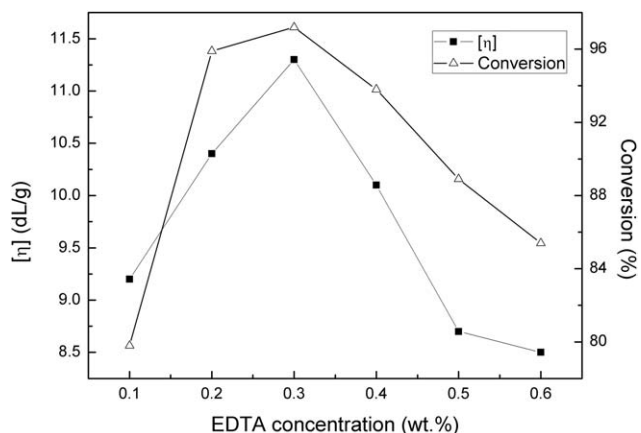


**Figure 12.** Effect of EDTA concentration on intrinsic viscosity and conversion.

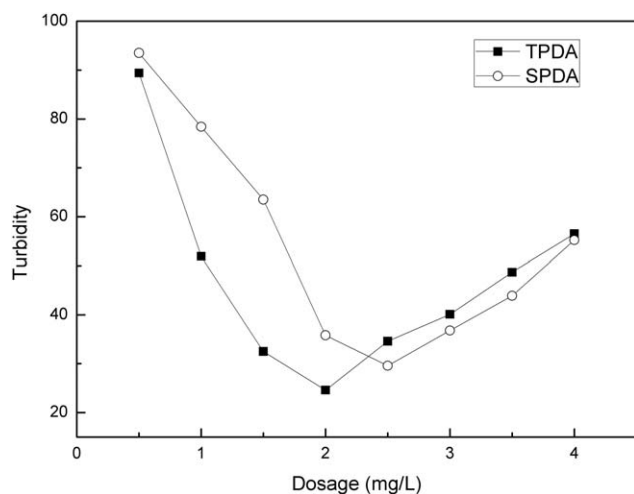


**Figure 13.** Effect of TPDA and SPDA dosage on turbidity.

was lower than  $2.0 \text{ mg L}^{-1}$  for TPDA and  $2.5 \text{ mg L}^{-1}$  for SPDA. During such periods, the higher intrinsic viscosity of TPDA bridged more efficiently than SPDA with less flocculant dose and lower turbidity. However, with excessive flocculants, the particle surface was almost completely covered and the steric repulsion between particles made efficient bridging effect almost impossible. Second, the electrical repulsion between particles was weakened; thus, flocs were formed with the charge neutralization effect of flocculant. Given its cationic block structure, TPDA should perform better in charge neutralization than SPDA. Therefore, both the optimum dosage and the corresponding turbidity of TPDA were lower than those of SPDA. Nevertheless, the presence of excessive flocculant causes mutual repulsion again and thus increases turbidity when the flocculant dose is further increased.<sup>28,29</sup>

## CONCLUSIONS

UV-initiated template polymerization was used to prepare CPAM with a high intrinsic viscosity and cationic block structure, which promote the efficient flocculation of kaolin suspensions. The FTIR and  $^1\text{H}$  NMR spectra show the functional groups of both AM and DMD units. The TGA thermograms not only indicate the favorable thermal stability but also the block structure of TPDA. An optimized product was obtained at an intrinsic viscosity of  $11.3 \text{ dL g}^{-1}$  and a conversion rate of 97.2% with a total monomer concentration of 20%, DMD concentration of 30%, initiator concentration of 0.045%, pH of 8, EDTA concentration of 0.3%, and UV irradiation of 90 min. The effect of DMD content on polymerization further confirmed the template effect and the cationic block structure. Given its high intrinsic viscosity and cationic block structure, TPDA performed better in kaolin flocculation than SPDA.

## ACKNOWLEDGMENTS

The authors are grateful for the financial support provided by the National Natural Science Foundation of China (Projects 21177164 and 21477010) and the 111 Project (Project No. B13041).

## REFERENCES

- Nasim, T.; Bandyopadhyay, A. *Sep. Purif. Technol.* **2012**, *88*, 87.
- Zhu, G.; Zheng, H.; Chen, W.; Fan, W.; Zhang, P.; Tshukudu, T. *Desalination* **2012**, *285*, 315.
- Zheng, H.; Zhu, G.; Jiang, S.; Tshukudu, T.; Xiang, X.; Zhang, P.; He, Q. *Desalination* **2011**, *269*, 148.
- Abdollahi, M.; Alamdari, P.; Koolivand, H.; Ziaee, F. *J. Polym. Res.* **2013**, *20*, 1.
- Bi, K.; Zhang, Y. *J. Appl. Polym. Sci.* **2012**, *125*, 1636.
- Wang, X.; Yue, Q.; Gao, B.; Si, X.; Sun, X.; Zhang, S. *J. Appl. Polym. Sci.* **2011**, *120*, 1496.
- Wang, X.; Yue, Q.; Gao, B.; Si, X.; Sun, X.; Zhang, S. *J. Polym. Res.* **2010**, *18*, 1067.
- Ondaral, S.; Usta, M.; Gumusderelioglu, M.; Arsu, N.; Balta, D. K. *J. Appl. Polym. Sci.* **2009**, *116*, 1157.
- Shang, H.; Zheng, Y.; Liu, J. *J. Appl. Polym. Sci.* **2011**, *119*, 1602.
- Polowiński, S. *Prog. Polym. Sci.* **2002**, *27*, 537.
- Zheng, H.; Ma, J.; Zhu, C.; Zhang, Z.; Liu, L.; Sun, Y.; Tang, X. *Sep. Purif. Technol.* **2014**, *123*, 35.
- Zheng, H.; Liao, Y.; Zheng, M.; Zhu, C.; Ji, F.; Ma, J.; Fan, W. *Sci. World J.* **2014**, *2014*, 1.
- Ma, J.; Zheng, H.; Tan, M.; Liu, L.; Chen, W.; Guan, Q.; Zheng, X. *J. Appl. Polym. Sci.* **2013**, *129*, 1984.
- Zhu, J.; Zheng, H.; Jiang, Z.; Zhang, Z.; Liu, L.; Sun, Y.; Tshukudu, T. *Desal. Water Treat.* **2013**, *51*, 2791.
- Zheng, H.; Sun, Y.; Zhu, C.; Guo, J.; Zhao, C.; Liao, Y.; Guan, Q. *Chem. Eng. J.* **2013**, *234*, 318.
- Lu, Y.; Deng, Z. *Practical Infrared Spectrum Analysis*; Electronic Industry Press: Beijing, **1989**.
- Wang, L.; Li, G.; Zhang, Y.; Xiao, H. *J. Appl. Polym. Sci.* **2013**, *130*, 4040.
- Yang, Z. L.; Gao, B. Y.; Li, C. X.; Yue, Q. Y.; Liu, B. *Chem. Eng. J.* **2010**, *161*, 27.
- Mapkar, J. A.; Iyer, G.; Coleman, M. R. *Appl. Surf. Sci.* **2009**, *255*, 4806.
- Abdel-Aziz, H. M.; Hanafi, H. A.; Abozahra, S. F.; Siyam, T. *Int. J. Polym. Mater.* **2011**, *60*, 89.
- Gong, L. X.; Zhang, X. F. *Express Polym. Lett.* **2009**, *3*, 778.
- Noppakundilgrat, S.; Nanakorn, P.; Jinsart, W.; Kiatkamjornwong, S. *Polym. Eng. Sci.* **2010**, *50*, 1535.
- Wu, Y.; Zhang, N. *J. Polym. Res.* **2009**, *16*, 647.
- Zhang, Y.; Wu, F.; Li, M.; Wang, E. *Acta Polym. Sin.* **2005**, *874*.
- Brand, F.; Dautzenberg, H.; Jaeger, W.; Hahn, M. *Angew. Makromol. Chem.* **1997**, *248*, 41.
- Seabrook, S. A.; Gilbert, R. G. *Polymer* **2007**, *48*, 4733.
- Zhen, H.-B.; Xu, Q.; Hu, Y.-Y.; Cheng, J.-H. *Chem. Eng. J.* **2012**, *209*, 547.
- Wang, J.-P.; Chen, Y.-Z.; Yuan, S.-J.; Sheng, G.-P.; Yu, H.-Q. *Water. Res.* **2009**, *43*, 5267.
- Yang, Z.; Yuan, B.; Huang, X.; Zhou, J.; Cai, J.; Yang, H.; Li, A.; Cheng, R. *Water Res.* **2012**, *46*, 107.